

Enhancing the static behavior of laminated composite plates using a porous layer

Yuan Yuan^{*1,3}, Ke Zhao^a and Kuo Xu⁴

School of Mechanical and Precision Instrument Engineering, Xi'an University of Technology,
Xi'an, 710048, China

(Received July 2, 2019, Revised August 7, 2019, Accepted August 26, 2019)

Abstract. The main aim of this paper is enhancing design of traditional laminated composite plates subjected to static loads. In this regard, this paper suggests embedding a lightweight porous layer in the middle of laminated composite as the core layer of the resulted sandwich plate. The static responses of the suggested structures with uniform, symmetric and non-symmetric porosity distributions are compared to optimize their design. Using the first order shear deformation theories, the static governing equations of the suggested laminated composite plates with a porous layer (LCPPL) rested on two-parameter foundation are obtained. A finite element method is also utilized to solve the governing equations of LCPPLs. Effects of laminated composite and porosity characteristics as well as geometry dimension, edges' boundary conditions and foundation coefficients on the static deflection and stress distribution of the suggested composite plates have been investigated. The results reveal that the use of core between the layers of laminated composites leads to a sharp reduction in the static deflections of LCPPLs. Furthermore, in compare with perfect cores, the use of porous core between the layers of laminated composite plates can offer a considerable reduction in structural weight without a significant difference in their static responses.

Keywords: lightweight structures; plate design; porosity effects; laminated composites; static loads

1. Introduction

Recently, the use of laminated composites in engineering applications has been widely attracted the attentions especially in sandwich structures where there are very large differences between the material properties between faces and core. These materials are utilized in several weight sensitive engineering applications like aerospace, civil, aeronautical industries, automotive design and marine (Salami and Dariushi, 2018, Vinson, 2001). The reasons of such extensive applications of laminated composites are their incredible design flexibility and managing their thermo-mechanical behavior which are provided by changing their arrangement sequence and fiber orientation in each layer (Vinson, 2001). Moreover, the use of laminated composites in sandwich structures usually improves the overall thermo-mechanical responses of laminated composites. In sandwich structures, the main role of core layer is providing adequate distance between the outer face sheets (Kamarian *et al.* 2017, Mohammadimehr *et al.* 2017, Moradi-Dastjerdi *et al.* 2017). Therefore, the use of foams or porous materials as a core layer could offer lighter sandwich structures with higher strength-to-weight ratio, absorption of energy, damping of vibration and more manageable thermo-mechanical properties (Rashidi *et al.*

2018). Due to the increased applications of these sandwich structures and in order to increase their effectiveness, a deep knowledge of their mechanical responses especially in terms of deflections and stress distributions are required.

As mentioned earlier, static response of engineering structures can play a main role in the design of most of such structures (Foroutan *et al.* 2012, Moradi-Dastjerdi *et al.* 2018, Moradi-Dastjerdi and Behdinan, 2019, Zargar *et al.* 2017). In this regard, finite element methods have been established their remarkable contributions (Ghanati and Safaei, 2019, Safaei *et al.* 2018, Shokri-Ooijghaz *et al.* 2019). During the last few years, mechanical analyses of sandwich structures have been presented by many researchers. Mantari *et al.* (2011) suggested a new HSDT with parabolic transvers shear strain distribution to analyze the bending responses of laminated composite plates. Rezaiee-Pajand *et al.* (2012) presented the static behavior of laminated composites sandwich plates in a framework of FEM with 13-noded elements. Thai *et al.* (2013) presented static, natural frequency and buckling responses of laminated composite plates using an isogeometric finite element method (FEM) formulation based on layerwise theory with the first order shear deformation theory (FSDT) in each layer. Ferreira *et al.* (2013) developed a method with the combination of GDQ technique and layer-wise method for the static and free vibration analyses of laminated composite plates. Xiang *et al.* (2015) proposed a n-order theory for the plates and compared the static responses of laminated composite sandwich plates under sinusoidal loads with other works. Belarbia *et al.* (2016) proposed a finite element solution with 4-noded elements and 52 degree of freedom to study

*Corresponding author, Associate Professor

E-mail: yuan yuan.xi.edu@gmail.com

^a M.Sc.

^b M.Sc.

the bending response of composite sandwich plates. They adopted the first and third order shear deformation theories for faces and core layers, respectively. Tian *et al.* (2016) proposed a new HSDT and presented the static bending and natural frequencies of sandwich plates with laminated composite faces and a soft core. Tornabene *et al.* (2017a) studied progressive damage effect in laminated composite sandwich shells by a generalized differential quadrature (GDQ) method. They also employed GDQ method to present the static analysis of laminated composite sandwich plates and shells (Tornabene *et al.* 2017b). Lin *et al.* (2018) developed a very accurate scaled boundary FEM solution based on 3D theory of elasticity for the mechanical analysis of laminated composite plates. Xiaohui *et al.* (2018) conducted static analysis of laminated composite plates by an analytical method based on Navier's method and a refined sinusoidal theory with zig-zag functions. Fantuzzi *et al.* (2018) provided a strong FEM to study the mechanical analysis of laminated composite plates and compared their results with the weak form results obtained from commercial FE packages. Zarei and Khosravifard (2019) developed a meshless method based on different orders of plate theories to study static responses of composite laminated plates.

Among the sandwich structures, different types of materials were suggested for the arrangement of layers in which the faces were usually stiffer than core. Thanks to the smooth variation of the volume fraction of components, functionally graded materials (FGMs) have become very popular and vastly utilized in the engineering structures (Jalali *et al.* 2018a, 2018b). The bending behavior of sandwich plates with FGM and homogenous layers have been presented using refined (Abdelaziz *et al.* 2011, Nguyen *et al.* 2015), five-unknown (Benbakhti *et al.* 2016) and four unknown (Driz *et al.* 2018) HSDTs. For the static study of the same plates, Neves *et al.* (2012) employed Murakami's Zig-Zag theory and a collocation method with radial basis functions. Furthermore, carbon nanotube (CNT)-reinforced nanocomposite materials are the other materials which were proposed for the face layers of sandwich structures (Pourasghar and Chen, 2019a, Qin *et al.* 2019, Safaei *et al.* 2019c). It should be mentioned that due to the astonishing properties of CNTs, a wide range of research on the mechanical behavior of CNT-reinforced structures (Pourasghar and Chen 2019b, 2019c, 2019d, 2016) have been carried out. Wang and Shen (2012) proposed this kind of sandwich plates with CNT-reinforced faces and studied the nonlinear deflections and natural frequencies of the proposed sandwich plates rested on elastic foundation. Jalali and Heshmati (2016) considered sandwich plates with multi-walled CNT-reinforced faces in circular tapered shapes and studied their buckling responses. Ebrahimi and Farazmandnia (2018) employed a semi-analytical method of differential transform to study the vibrational behavior of sandwich Timoshenko beams with CNT-reinforced faces in thermal environment. Mehar and Panda (2018) developed HSDT based FEM and presented the nonlinear stress distributions of sandwich shallow shells with temperature-dependent CNT-reinforced faces. The effects of defects and agglomeration of CNTs on

the static bending and stress distributions of sandwich plates with CNT-reinforced faces were studied in (Mirzaalian *et al.* 2019, Moradi-Dastjerdi and Aghadavoudi 2018).

Porous materials are usually utilized in engineering structures to improve their thermo-mechanical responses. In the manufacturing process, voids can be created inside materials because of some technical issues such as low process pressure. Voids can also be intentionally formed to improve the performance of manufactured foams (Rashidi *et al.* 2018). As mentioned before, the use of porous material can considerably reduce the structural weights. As a pioneer work, the effect of embedding porosity on the static behavior of axisymmetric plates were studied in (Magnucka-Blandzi, 2008). Using 3D theory of elasticity in combination with DQM, Rad *et al.* (2017) investigated the static behavior of circular porous plates with variable thickness rested on Horvath-Colasanti type foundations. Nguyen *et al.* (2018) employed HSDT based FEM with polygonal elements to investigate the deflections of porous FGM plates under static and dynamic loads. The effect of embedding porosity on the buckling responses of CNT-reinforced (Guessas *et al.* 2018) and on the static responses of graphene-reinforced (Polit *et al.* 2019) plates were also investigated using the first and higher order theories of plates, respectively. Moreover, the buckling behavior of sandwich plates consisting metallic faces and porous core was presented in (Chen *et al.* 2019). Safaei *et al.* (2019a) considered a uniform distribution for porosities along the whole thickness of sandwich plates with CNT-reinforced faces and studied thermal and mechanical buckling behaviors. Setoodeh *et al.* (2019) employed GDQ method and conducted the vibrational behavior of sandwich plates consisting a two piezoceramics layers, two CNT-reinforced layers and one porous core. Safaei *et al.* (2019b) also proposed sandwich plates with a porous core and CNT-reinforced faces and presented their thermoelastic static deflections and stress distributions.

This paper suggests embedding a porous layer between the layers of laminated composite plates to enhance the mechanical responses of traditional laminated composite plates. Three different profiles for porosity distribution in the porous layer have been considered. Specifically, the deflection and stress distributions of the resulted sandwich plates called LCPPLs rested on a two-parameter foundation are presented. In this regard, the static governing equations are obtained based on FSDT. Then, the obtained equations are solved by a developed finite element method. Using the developed solution method, the effects of laminated composite and porosity characteristics as well as geometry dimension, edges' boundary conditions and foundation coefficients on the static responses of the suggested LCPPLs have been presented.

2. Modeling of porous sandwich plate

The schematic figure of the suggested LCPPL rested on a two-parameter foundation with normal k_1 and shear k_2 effects is shown in Fig. 1. The plate is assumed to be subjected to uniform pressure f_0 . The laminated composite layers are assumed to be made of Graphite/Epoxy (Gr/Ep)

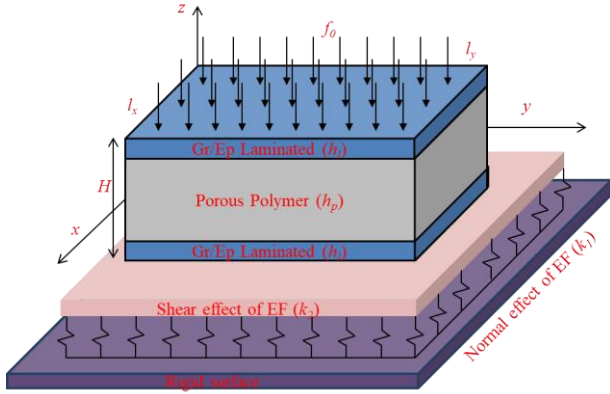


Fig. 1 The schematic figure of the suggested laminated composite plates with a porous layer

and the porous layer is made of pure epoxy. As depicted in Fig. 1, l_x , l_y and H are the length, width and total thickness of LCPPL, respectively. The fiber orientations of laminated composite layers are assumed to be symmetric and changed from α_1 to α_{n_l} from the inner faces to outer faces which shown as $[\alpha_1, \alpha_2, \dots, \alpha_{n_l}]$. n_l is the number lamina in the laminated composite layers. In addition, uniform, symmetric (Sym.) and non-symmetric (Non-Sym.) porosity distributions are assumed for the porous core.

The elastic modulus E_p and Poisson's ratio ν_p of porous core can be estimated by closed-cell Gaussian random field models as follows (Zhao *et al.* 2019):

$$E_p = (1 - V_p)E, \nu_p = (1 - V_p)\nu \quad (1)$$

where E and ν are the maximum values of elastic modulus and Poisson's ratio which are related to a core without porosity. By the definition of p_0 which indicates the porosity parameter of the core layer, the volume of porosities V_p for the three prescribed porosity distributions can be defined as (Zhao *et al.* 2019):

$$\text{Uniform: } V_p = p_0 \Phi, \quad \Phi = \frac{1}{p_0} \left[1 - \left(\frac{2}{\pi} \sqrt{1 - p_0} - \frac{2}{\pi} + 1 \right)^2 \right] \quad (2)$$

$$\text{Sym.: } V_p = p_0 \cos(\pi z / h_p) \quad (3)$$

$$\text{Non-Sym.: } V_p = p_0 \cos\left(\frac{\pi z}{4h_p} + \frac{\pi}{4}\right) \quad (4)$$

The distributions of V_p along the thickness of porous core are illustrated in Fig. 2.

3. Governing equations

3.1 Basic equations

In this paper, a five-unknown first order shear deformation theory is employed for the estimation of displacement field in the suggested laminated composite

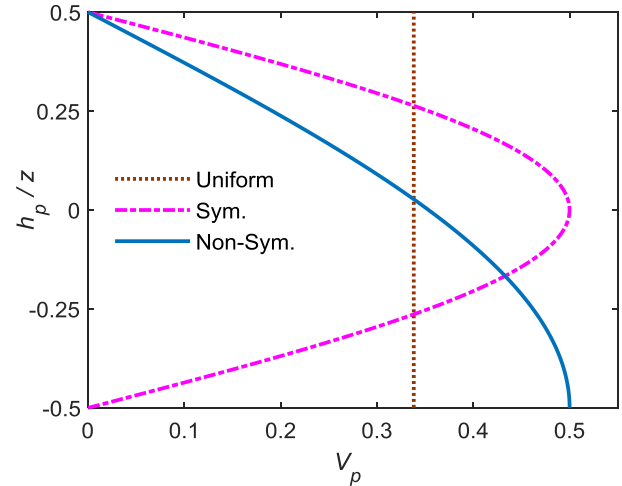


Fig. 2 The distributions of the volume of porosities along the thickness of porous core

plates with a porous layer because of its acceptable accuracy for thin to moderately thick plates and computational cost issues. According to the employed FSDT, the displacement components of u , v and w can be expressed with three mid-plane unknowns of u_0 , v_0 and w_0 , and two mid-plane normal rotational unknowns of θ_x and θ_y . This FSDT is determined as follows (Mohammadsalehi *et al.* 2017, Reddy 2004):

$$\begin{aligned} u &= u_0(x, y) + z\theta_x(x, y) \\ v &= v_0(x, y) + z\theta_y(x, y) \\ w &= w_0(x, y) \end{aligned} \quad (5)$$

Considering the linear parts, the strain components of the suggested plates can be described as follows (Reddy, 2004):

$$\begin{aligned} \epsilon_{xx} &= \frac{\partial u}{\partial x}, \epsilon_{yy} = \frac{\partial v}{\partial y}, \gamma_{xy} = \frac{\partial u}{\partial y} + \frac{\partial v}{\partial x} \\ \gamma_{xz} &= \frac{\partial u}{\partial z} + \frac{\partial w}{\partial x}, \gamma_{yz} = \frac{\partial v}{\partial z} + \frac{\partial w}{\partial y} \end{aligned} \quad (6)$$

The strain vector of plates can be divided to in-plane ϵ_b and out-of-plane γ strain vectors. Considering Eqs. (5) and (6), these vectors are given below:

$$\epsilon_b = \begin{Bmatrix} \partial u_0 / \partial x \\ \partial v_0 / \partial y \\ \partial u_0 / \partial y + \partial v_0 / \partial x \end{Bmatrix} + z \begin{Bmatrix} \partial \theta_x / \partial x \\ \partial \theta_y / \partial y \\ \partial \theta_x / \partial y + \partial \theta_y / \partial x \end{Bmatrix}, \quad (7)$$

$$\gamma = \begin{Bmatrix} \theta_x + \partial w_0 / \partial x \\ \theta_y + \partial w_0 / \partial y \end{Bmatrix}$$

They can also be written as:

$$\epsilon_b = \{\epsilon_{xx} \quad \epsilon_{yy} \quad \gamma_{xy}\}^T = \epsilon_0 + z\epsilon_1, \quad \gamma = \{\gamma_{xz} \quad \gamma_{yz}\}^T \quad (8)$$

Furthermore, the constitutive equations for laminated composite and porous layers can relate in-plane σ and

out-of-plane $\boldsymbol{\tau}$ stress vectors to corresponding strain vectors as follows (Reddy 2004):

$$\begin{cases} \sigma_x \\ \sigma_y \\ \sigma_{xy} \end{cases} = \begin{bmatrix} D_{11} & D_{12} & D_{16} \\ D_{12} & D_{22} & D_{26} \\ D_{26} & D_{26} & D_{66} \end{bmatrix} \begin{cases} \varepsilon_x \\ \varepsilon_y \\ \gamma_{xy} \end{cases} \quad (9)$$

$$\begin{cases} \tau_{xz} \\ \tau_{yz} \end{cases} = \frac{5}{6} \begin{bmatrix} D_{55} & D_{45} \\ D_{45} & D_{44} \end{bmatrix} \begin{cases} \gamma_{xz} \\ \gamma_{yz} \end{cases}$$

where $5/6$ is appeared because of the utilized FSDT for the suggested plate as shear correction factor. Eq. (9) can be rewritten in vector terms as follows:

$$\boldsymbol{\sigma} = \mathbf{D}_b \boldsymbol{\varepsilon}_b, \quad \boldsymbol{\tau} = \frac{5}{6} \mathbf{D}_s \boldsymbol{\gamma}, \quad \mathbf{D} = \begin{bmatrix} \mathbf{D}_b & 0 \\ 0 & \mathbf{D}_s \end{bmatrix} \quad (10)$$

The components of elastic constant matrix \mathbf{D} for isotropic porous core and laminated composite layers are determined in Appendix.

The total energy of the plate is a summation of strain energy, work done by external uniform pressure, and the energy of the two-parameter foundation. This energy function for the suggested LCPPL can be determined as follows (Moradi-Dastjerdi and Momeni-Khabisi, 2016)

$$U = \frac{1}{2} \int_V [\boldsymbol{\varepsilon}_b^T \boldsymbol{\sigma} + \boldsymbol{\gamma}^T \boldsymbol{\tau}] dV + \int_{\Omega} f_0 w dV + \frac{1}{2} \int_A [k_1 w^2 + k_2 [(\partial w / \partial x)^2 + (\partial w / \partial y)^2]] dA \quad (11)$$

where Ω and V are the top or downer face area and the total volume of LCPPL.

3.2 FEM formulations

According to the concept of FEM, the displacement field can be estimated by some point called nodes which are determined by meshing the domain. For the suggested LCPPL, the exact displacement field \mathbf{d} is approximated in n predefined nodes d_i using the values of finite element shape functions ψ_i as follows:

$$\mathbf{d} = \sum_{i=1}^n \psi_i d_i \quad (12)$$

where four-node rectangular elements with bilinear shape functions ψ_i are employed. Considering the employed FSDT in Eq. (5) with its five unknowns, the nodal approximated values of displacement at i^{th} node can be determined as follows (Safaei *et al.* 2019d):

$$d_i = [u_{0i}, v_{0i}, w_{0i}, \theta_{xi}, \theta_{yi}]^T \quad (13)$$

Substituting Eq. (12) into Eq. (8) with respect to Eq. (7) regenerates strain vectors in FEM formulations as follows

$$\boldsymbol{\varepsilon}_b = \{\mathbf{H}_0 + z \mathbf{H}_1\} \mathbf{U}, \quad \boldsymbol{\gamma} = \mathbf{H}_s \mathbf{U} \quad (14)$$

where:

$$\mathbf{H}_s = \begin{bmatrix} 0 & 0 & \partial \psi_i / \partial x & \psi_i & 0 \\ 0 & 0 & \partial \psi_i / \partial y & 0 & \psi_i \end{bmatrix},$$

$$\mathbf{H}_0 = \begin{bmatrix} \partial \psi_i / \partial x & 0 & 0 & 0 & 0 \\ 0 & \partial \psi_i / \partial y & 0 & 0 & 0 \\ \partial \psi_i / \partial y & \partial \psi_i / \partial x & 0 & 0 & 0 \end{bmatrix}, \quad (15)$$

$$\mathbf{H}_1 = \begin{bmatrix} 0 & 0 & 0 & \partial \psi_i / \partial x & 0 \\ 0 & 0 & 0 & 0 & \partial \psi_i / \partial y \\ 0 & 0 & 0 & \partial \psi_i / \partial y & \partial \psi_i / \partial x \end{bmatrix}$$

Introducing Eqs. (10), (12) and (13) into the total energy function (Eq. 15) results in:

$$U = \frac{1}{2} \int_{\Omega} \mathbf{d}^T \left\{ \mathbf{H}_0^T \bar{\mathbf{D}}_0 \mathbf{H}_0 + \mathbf{H}_0^T \bar{\mathbf{D}}_1 \mathbf{H}_1 + \mathbf{H}_1^T \bar{\mathbf{D}}_1 \mathbf{H}_0 + \mathbf{H}_1^T \bar{\mathbf{D}}_2 \mathbf{H}_1 + \mathbf{H}_s^T \bar{\mathbf{D}}_s \mathbf{H}_s \right\} \mathbf{d} d\Omega + \int_{\Omega} \mathbf{d}^T \mathbf{H}_n^T f d\Omega + \frac{1}{2} \int_{\Omega} \mathbf{d}^T \left\{ \mathbf{H}_n^T k_1 \mathbf{H}_n + \mathbf{H}_{s2}^T k_2 \mathbf{H}_{s2} \right\} \mathbf{d} d\Omega \quad (16)$$

where

$$(\bar{\mathbf{D}}_0, \bar{\mathbf{D}}_1, \bar{\mathbf{D}}_2) = \int_{-h/2}^{h/2} \mathbf{D}_b(1, z, z^2) dz, \quad \bar{\mathbf{D}}_s = \frac{5}{6} \int_{-h/2}^{h/2} \mathbf{D}_s dz \quad (17)$$

$$\mathbf{H}_n = [0 \quad 0 \quad \psi_i \quad 0 \quad 0],$$

$$\mathbf{H}_{s2} = \begin{bmatrix} 0 & 0 & \partial \psi_i / \partial x & 0 & 0 \\ 0 & 0 & \partial \psi_i / \partial y & 0 & 0 \end{bmatrix} \quad (18)$$

Noted that the coupling stiffness matrix is zero $\bar{\mathbf{D}}_1 = 0$ for symmetric LCPPLs. The minimizing of total energy function Eq. (16) leads to the following system of static governing equations for the suggested LCPPL:

$$\mathbf{Kd} = \mathbf{F} \quad (19)$$

where the global stiffness matrix \mathbf{K} and force vector \mathbf{F} are determined as follows:

$$\mathbf{K} = \int_{\Omega} \left\{ \mathbf{H}_0^T \bar{\mathbf{D}}_0 \mathbf{H}_0 + \mathbf{H}_0^T \bar{\mathbf{D}}_1 \mathbf{H}_1 + \mathbf{H}_1^T \bar{\mathbf{D}}_1 \mathbf{H}_0 + \mathbf{H}_1^T \bar{\mathbf{D}}_2 \mathbf{H}_1 + \mathbf{H}_s^T \bar{\mathbf{D}}_s \mathbf{H}_s \right\} d\Omega + \int_{\Omega} \left\{ \mathbf{H}_n^T k_1 \mathbf{H}_n + \mathbf{H}_{s2}^T k_2 \mathbf{H}_{s2} \right\} d\Omega \quad (20)$$

$$\mathbf{F} = \int_{\Omega} \mathbf{H}_n^T f d\Omega \quad (21)$$

4. Results and discussions

In the following simulations of the suggested LCPPL, fully clamped (CCCC) square plates subjected to a uniform pressure of $f_0=10$ kPa with $l_x/h_p = 10$, $l_x/h_l = 100$, $K_1=0$ and $K_2=0$ are considered unless otherwise stated. It is assumed that the laminated composite layers are made of Graphite/Epoxy (Gr/Ep) and core is made of pure epoxy.

Table 1 The normalized central deflections of square simply supported isotropic plates

l_x/H	Method	\hat{w}
10	FEM (Reddy, 1993)	4.770
	Finite Point (Ferreira <i>et al.</i> 2003)	4.7866
	Collocation (Ferreira <i>et al.</i> 2009)	4.7912
	Meshless (Moradi-Dastjerdi <i>et al.</i> 2016)	4.7864
	Exact (Akhras <i>et al.</i> 1994)	4.791
	Present	4.7901
20	FEM (Reddy, 1993)	4.570
	Finite Point (Ferreira <i>et al.</i> 2003)	4.6132
	Collocation (Ferreira <i>et al.</i> 2009)	4.6254
	Meshless (Moradi-Dastjerdi <i>et al.</i> 2016)	4.6274
	Exact (Akhras <i>et al.</i> 1994)	4.625
	Present	4.6242
100	FEM (Reddy, 1993)	4.482
	Finite Point (Ferreira <i>et al.</i> 2003)	4.5737
	Collocation (Ferreira <i>et al.</i> 2009)	4.5716
	Meshless (Moradi-Dastjerdi <i>et al.</i> 2016)	4.5765
	Exact (Akhras <i>et al.</i> 1994)	4.572
	Present	4.5710

The utilized material properties are as follows (Akhras and Li 2010):

Gr/Ep: $E_{11}=181$ GPa, $E_{12}=E_{13}=10.3$ GPa, $G_{12}=G_{13}=7.179$ GPa, $G_{23}=2.87e9$ GPa, $\nu_{12}=\nu_{13}=0.28$, $\nu_{23}=0.33$

Epoxy: $E=4.5$ GPa, $\nu=0.4$

Moreover, the following normalized parameters for foundation coefficients K_1 , K_2 and deflections \hat{w} are utilized in our reported results:

$$K_1 = k_1 l_x^4 / D, \quad K_2 = k_2 l_x^4 / D \quad \text{and} \quad \hat{w} = 100 E H_0^3 w / (f_0 l_x^4) \quad (22)$$

where

$$D = E h^3 / 12(1-\nu^2) \quad \text{and} \quad H_0 = 0.1 m \quad (23)$$

4.1 Validation of models

Due to the lack of results on the static analysis of the suggested LCPPL, the accuracy of the developed FEM could be examined by comparing the static results of isotropic plates with those existed in literatures. Therefore, square simply supported isotropic plates subjected to uniform load with $\nu=0.25$ and different thicknesses have been considered. Our results have been compared with the exact results reported in (Akhras *et al.* 1994) as well as the results of other numerical methods (Ferreira *et al.* 2003, Ferreira *et al.* 2009, Moradi-Dastjerdi *et al.* 2016, Reddy, 1993) in Table 1. The results show that the developed FEM has a very good accuracy because of its agreement with the reported results of normalized central deflections $\bar{w} = 100 E H^3 w / (f_0 l_x^4)$.

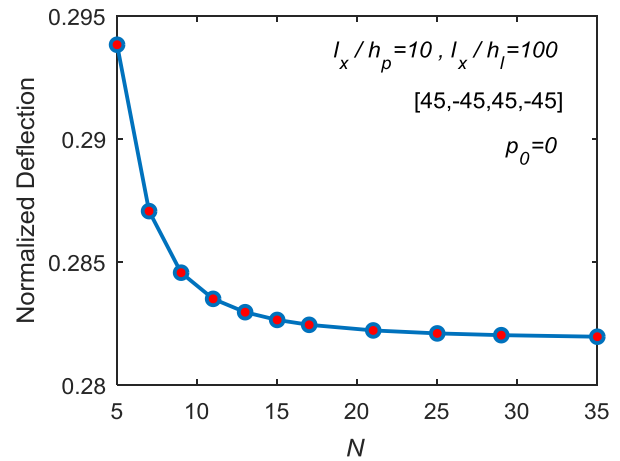


Fig. 3 \hat{w} of LCPPL as a function of element numbers in each direction

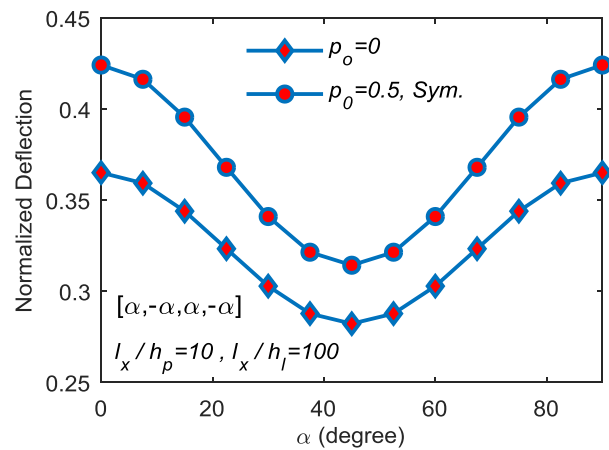


Fig. 4 \hat{w} as a function of fibre orientation in the laminated faces of LCPPL

Due to the lack of available results for the same LCPPL, this section is enhanced by the examination of convergence of the developed FEM in Fig. 3. This figure illustrates the normalized central deflections \hat{w} of LCPPLs with four-layer laminated faces of $\alpha=\pm 45$ versus element numbers in each direction N . It is observed that by adopting the element arrangement of 21×21 , the value of deflection is almost equal to the values of deflection determined using higher number of elements which means the results are converged. Hence, this element arrangement is adopted for the following simulations.

4.2 Deflection of the suggested LCPPL

First, the effects of laminated composite parameters including the number of layers and the orientation of fibres in each layer are investigated on the deflection of the suggested LCPPL. Fig. 4 illustrates the normalized central deflections of LCPPLs with four-layer laminated composite faces $[\alpha, -\alpha, \alpha, -\alpha]$ as a function of α from 0 to 90 degrees for plates with a symmetric porous core $\rho_0=0.5$ and a core without porosity $\rho_0=0$. The figure shows that the use of

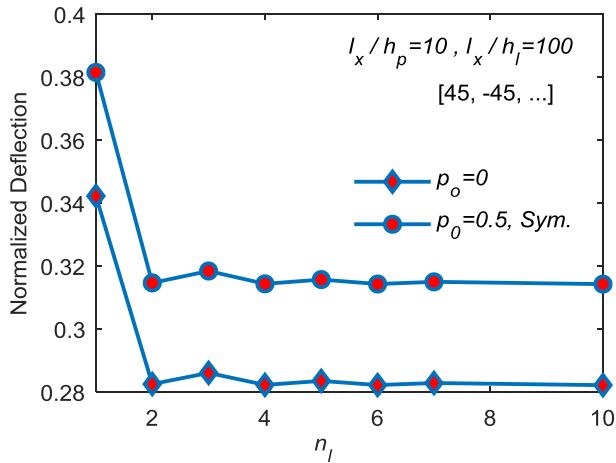


Fig. 5 \hat{w} as a function of the numbers of layers in the laminated faces of LCPPL

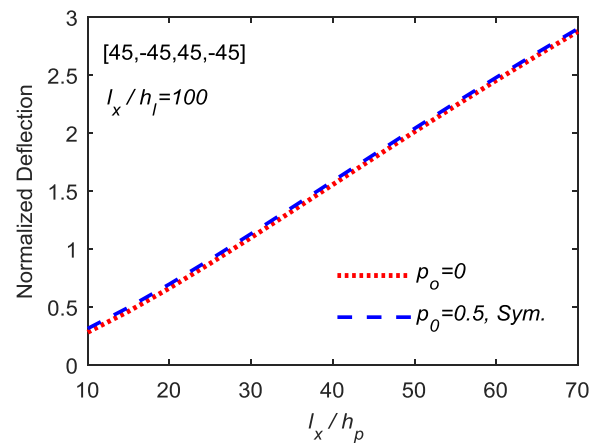


Fig. 7 \hat{w} as a function of l_x/h_p for LCPPLs with $l_x/h_l=100$

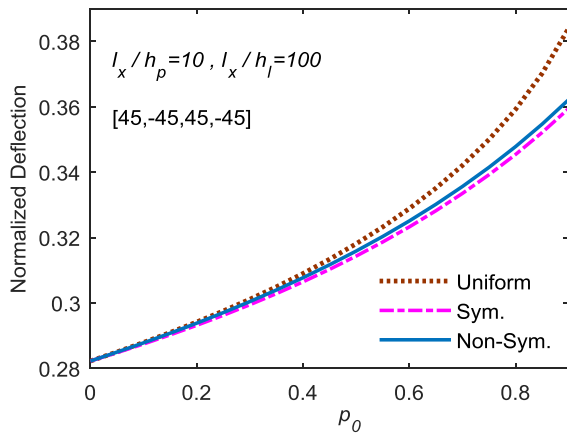


Fig. 6 \hat{w} as a function of porosity parameter in LCPPL with uniform, symmetric and non-symmetric porous core

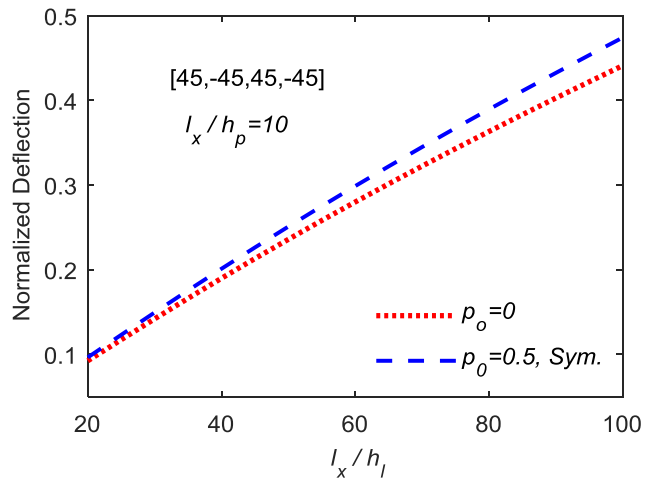


Fig. 8 \hat{w} as a function of l_x/h_l for LCPPLs with $l_x/h_p=10$

porous core results in higher values of deflections. Moreover, the use of laminated composite faces with $\alpha=\pm 45$ offers LCPPLs with the minimum deflections. However, laminate composite faces with $\alpha=0$ or 90 provide LCPPL with less structural stiffness and the highest deflections.

Fig. 5 also shows the central deflections of LCPPLs as a function of the number of layers in laminated faces with $\alpha=\pm 45$. It can be seen that the use of laminated faces with only a single layer results in the biggest deflections. However, the increase of n_l from one leads to a dramatically reduction in the deflections. The reason is that the capability of plates for loading transfer in two directions was improved. The same condition was observed in Fig. 4 for $\alpha=0$ or 90 . Moreover, laminated faces with odd numbers of layers ($n_l=1, 3, 5, \dots$) have higher deflections than those with even numbers ($n_l=2, 4, 6, \dots$). It also observed that the addition of layers after $n_l=4$ (especially for even numbers) has no considerable effect on the reduction of LCPPL deflections.

The effects of porosity characteristics including porosity parameters (volume) p_0 and porosity distribution are shown in Fig. 6. It can be seen that at the same values of p_0 , the suggested LCPPLs with symmetric and uniform porous

Table 2 \hat{w} for the suggested LCPPLs with symmetric porous core and [45, -45, 45, -45] laminated faces

B.C.	K_1, K_2	$l_y/l_x=1$		$l_y/l_x=2$	
		$p_0=0$	$p_0=0.5$	$p_0=0$	$p_0=0.5$
CCCC	(0,0)	0.2822	0.3143	0.5127	0.56465
	(50,0)	0.2795	0.3109	0.5033	0.55325
	(0,5)	0.2769	0.3077	0.5010	0.55066
CSCS	(0,0)	0.3504	0.3858	1.0197	1.0873
	(50,0)	0.3462	0.3808	0.9853	1.0481
	(0,5)	0.3424	0.3761	0.9780	1.0399
SSSS	(0,0)	0.4413	0.4745	1.0910	1.1535
	(50,0)	0.4348	0.4669	1.0515	1.1092
	(0,5)	0.4289	0.4601	1.0435	1.1004

cores have the lowest and highest values of deflections, respectively. Moreover, the use of porous cores leads to LCPPL with higher deflections. The increase of porosity parameter from $p_0=0$ to $p_0=0.6$ leads to slight increases in the deflections of LCPPLs with all the three profiles of porosity distributions; however, for $p_0>0.6$, there is a

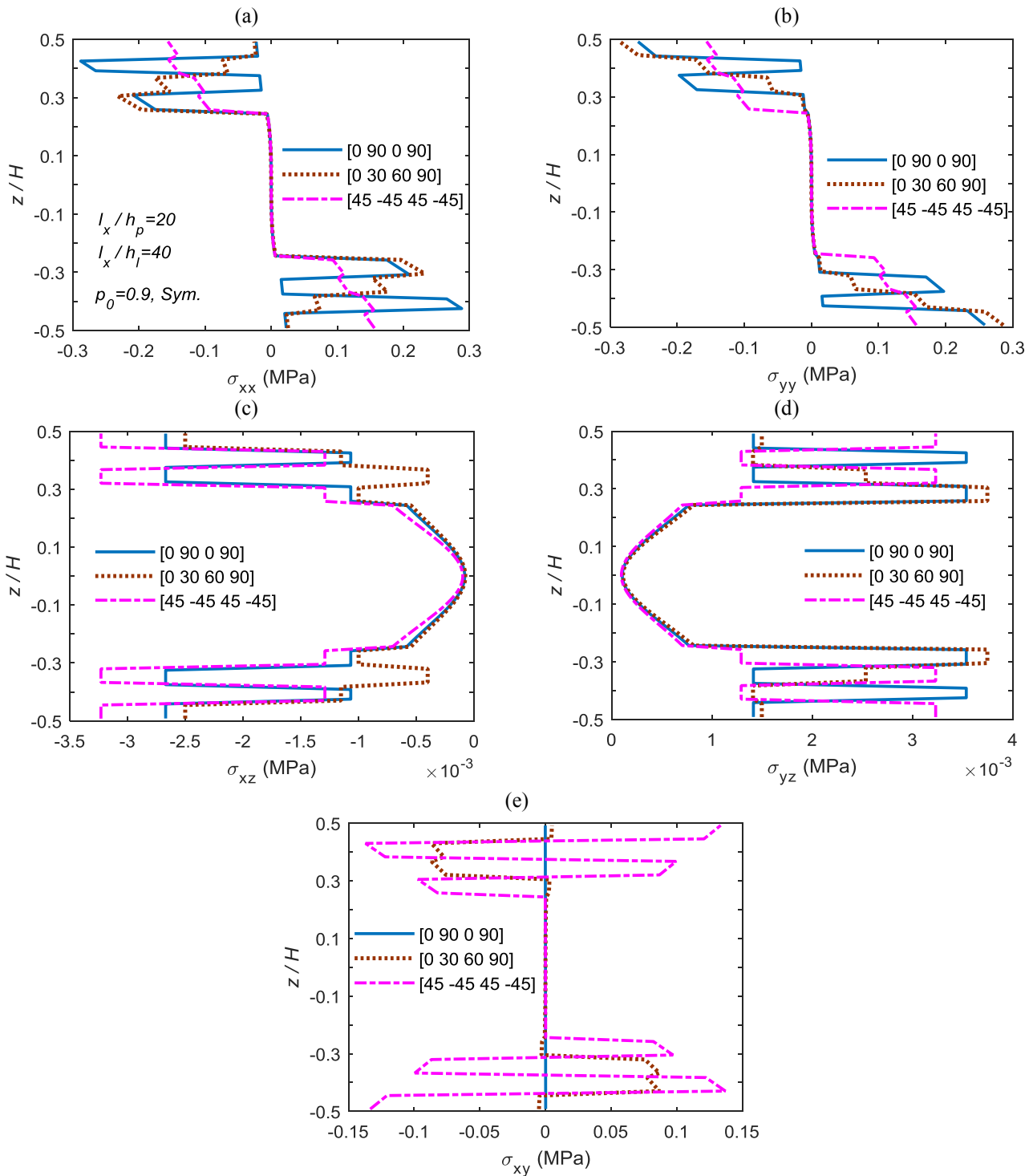


Fig. 9 Stress distributions of through the thicknesses of LCPPLs with different fibre orientation arrangements

significant difference in the deflections of the plates with uniform porous core and those with both symmetric and non-symmetric porous cores.

For the suggested LCPPL, the effects of core thickness and laminated faces thickness on deflections are shown in Figs. 7 and 8, respectively. For the plates with $l_x/h_l = 100$, Fig. 7 shows that the increase of l_x/h_p which means the reduction of core thickness, leads to increase in the central deflections of the suggested plates with both porous core $p_0=0.5$ and a core without porosity $p_0=0$. Moreover, for the

plates with $l_x/h_p = 10$, Fig. 8 shows that the increase of l_x/h_l which means the use of thinner laminated faces leads to dramatically increases of deflections. The effect of porosity on the deflections is increased by the decrease of the thickness of laminated faces. However, both figures show that the effect of porosity parameter on the deflections of the suggested LCPPLs is much lower than the thicknesses of LCPPL's layers. This observation discloses that the weight of LCPPL can be easily reduced without a considerable increase in their static deflections. It also can

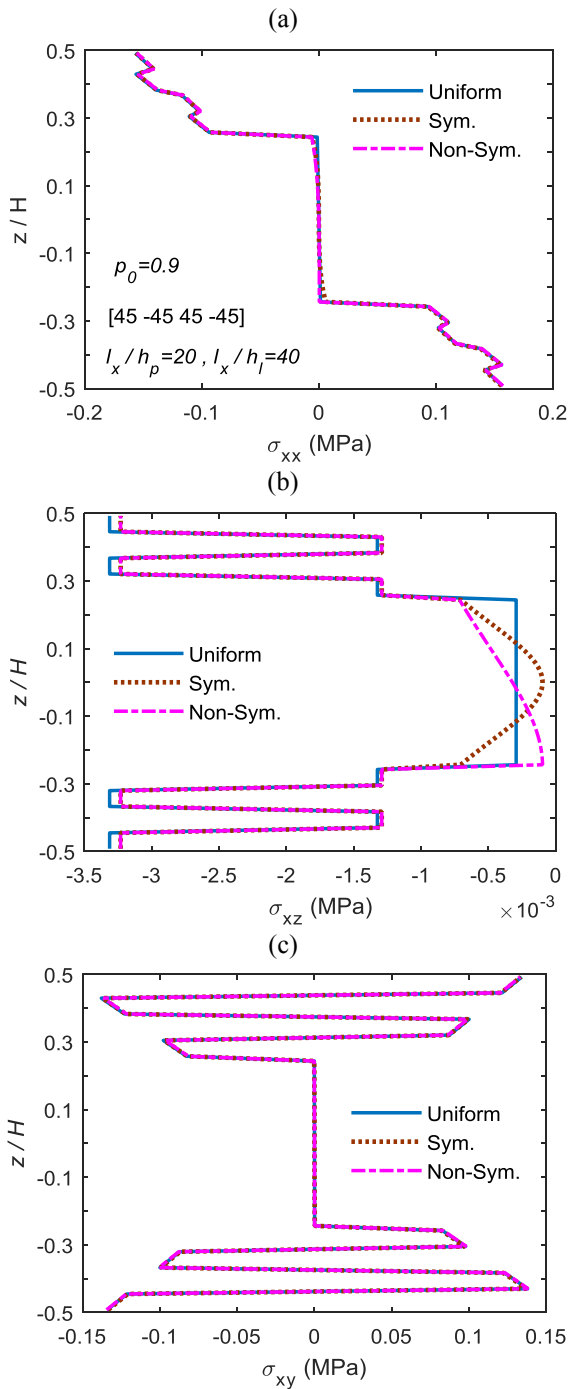


Fig. 10 Stress distributions of through the thicknesses of LCPPs with the different profiles of porosity

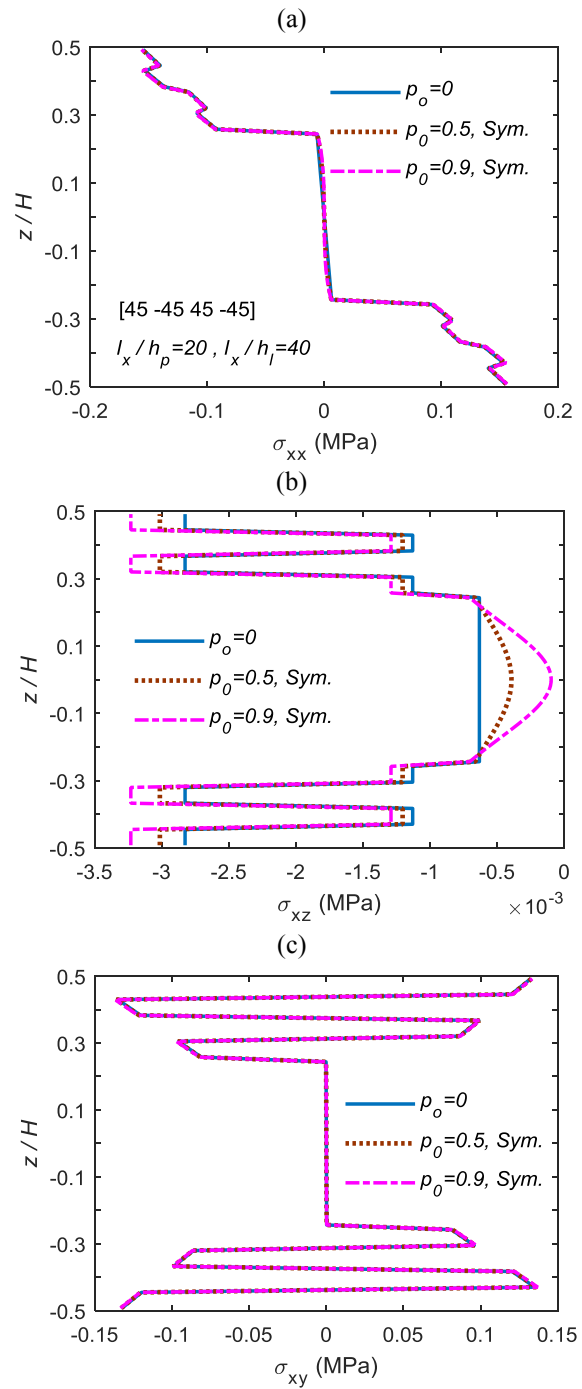


Fig. 11 Stress distributions of through the thicknesses of LCPPs with the different values of porosity parameter

be concluded that the use of core (with or without porosity) between the layers of laminated composites leads to a sharp reduction in the static deflections of the resulted LCPPs.

The effects of the length, the boundary conditions (here S, C and F are respected the edges with simply supported, clamped and free constrain, respectively) and foundation coefficients on the deflection of the suggested LCPP are shown in Table 2. The results show that rectangular plates have much higher deflection than corresponding square ones especially in plates with CSCS boundary conditions. Moreover, among the considered boundary

conditions, the highest and the lowest deflections are observed in fully simply supported and clamped LCPPs. In terms of foundation coefficients, the shear effect K_2 of foundation has bigger influence than the normal one K_1 on decreasing the deflections.

4.3 Stress distribution in the suggested LCPP

For the stress distributions of the suggested LCPP, clamped square plates subjected to a uniform pressure of $f_0=10$ kPa with $l_x/h_p = 20$, $l_x/h_l = 40$, $K_1=0$ and $K_2=0$ are considered.

The effect of fibre orientations on the static results of LCPPLs with four-layer laminated composites of [0 90 0 90], [0 30 60 90] and [45 -45 45 -45] are shown in Fig. 9. It can be seen that the core and laminated composite layers have the lowest and highest values of stresses, respectively.

It is observed that normal stresses are smoothly changed between [45 -45 45 -45] laminated layers; however, their sharp changes are observed between the [0 90 0 90] laminated layers. A comparison between Figs. 9a and 9b discloses that the layers with the same fibre orientations have almost the same normal stress values. Among the considered LCPPLs, the plates with [0 30 60 90] and [45 -45 45 -45] laminated layers have the lowest and highest values of out-of-plane shear stresses, respectively. But, the lowest values of in-plane shear stress are observed for the plate with [45 -45 45 -45] laminated layers. Furthermore, in [45 -45 45 -45] LCPPL, the equal values of normal stresses ($\sigma_{xx} = \sigma_{yy}$) and out-of-plane shear stresses ($\tau_{xz} = \tau_{yz}$) are observed due to the symmetric arrangement of fibre orientation in both x and y directions. Figs. 10 and 11 also show the effect of porosity distribution and parameter on the static responses of [45 -45 45 -45] LCPPLs, respectively. The figures show that both porosity characteristics have an insignificant effect on the in-plane stresses of the considered plates which reveals that the use of porous core offers stable conditions in terms of in-plane normal and shear stresses. The reason is that the values of in-plane stresses are directly related to the stiffness of each layer. As mentioned in Section 4, the Young's modulus of (perfect or porous) core is much less than Young's modulus of laminated composites. Furthermore, these two parameters of porous core have a significant effect on the out-of-plane shear stress distributions. The distribution of τ_{xz} (and τ_{yz}) are completely similar to the profile and volume of porosities in core layer.

5. Conclusions

This paper suggested embedding a porous layer in the middle of laminated composite layers to enhance the static behavior of traditional laminated composite plates. The static governing equations of the suggested LCPPL rested on two-parameter foundation were derived and investigated in a framework of FSDT and FEM to present their deflection and stress distributions. The following results were observed in our investigations:

- Embedding core (with or without porosity) between the layers of laminated composites leads to a sharp reduction in the static deflections of the resulted LCPPLs.
- In compare with perfect cores, the use of porous cores between the layers of laminated composite plates can offer a considerable reduction in structural weight without a significant difference in their static responses.
- The minimum and maximum deflections were observed for LCPPLs with fibre orientations of only $\alpha=\pm 45$ and $\alpha=0$ (or 90), respectively.
- The increase of porosity parameter from $p_0=0$ to $p_0=0.6$ leads to slight increases in the deflections of LCPPLs.

- The addition of layers after $n_l=4$ has no considerable effect on the reduction of LCPPL deflections.
- A smooth variation of normal stresses between the layers of laminated faces are observed in [45 -45 45 -45] LCPPLs.

References

- Abdelaziz, H.H., Atmane, H.A., Mechab, I., Boumia, L., Tounsi, A and El Abbas, A.B. (2011), "Static Analysis of Functionally Graded Sandwich Plates Using an Efficient and Simple Refined Theory", *Chinese J. Aeronaut.*, **24**(4), 434–448. [https://doi.org/10.1016/S1000-9361\(11\)60051-4](https://doi.org/10.1016/S1000-9361(11)60051-4).
- Akhras, G. and Li, W.C., (2010), "Three-dimensional thermal buckling analysis of piezoelectric antisymmetric angle-ply laminates using finite layer method", *Compos. Struct.*, **92**(1), 31–38. <https://doi.org/10.1016/j.compstruct.2009.06.010>.
- Akhras, G., Cheung, M. and Li, W. (1994), "Finite strip analysis for anisotropic laminated composite plates using higher-order deformation theory", *Compos. Struct.*, **52**, 471–477. [https://doi.org/https://doi.org/10.1016/0045-7949\(94\)90232-1](https://doi.org/https://doi.org/10.1016/0045-7949(94)90232-1).
- Belarbia M-O, Tatib A, Ounisc H. and Benchabane, A. (2016), "Development of a 2D isoparametric finite element model based on the layerwise approach for the bending analysis of sandwich plates", *Struct. Eng. Mech.*, **57**(3), 473–506. <https://doi.org/10.12989/sem.2016.57.3.473>.
- Benbakhti, A., Bouiadjra, M. B., Retiel, N. and Tounsi, A. (2016), "A new five unknown quasi-3D type HSDT for thermomechanical bending analysis of FGM sandwich plates", *Steel Compos. Struct.*, **22**(5), 975–999. <https://doi.org/10.12989/scs.2016.22.5.975>.
- Chen, D., Yang, J. and Kitipornchai, S. (2019), "Buckling and bending analyses of a novel functionally graded porous plate using Chebyshev-Ritz method", *Arch. Civ. Mech. Eng.*, **19**(1), 157–170. <https://doi.org/10.1016/j.acme.2018.09.004>.
- Driz, H., Benchohra, M., Bakora, A., Benachour, A., Tounsi, A. and Bedia, E.A.A. (2018), "A new and simple HSDT for isotropic and functionally graded sandwich plates", *Steel Compos. Struct.*, **26**(4), 387. <https://doi.org/10.12989/scs.2018.26.4.387>.
- Ebrahimi, F. and Farazmandnia, N. (2018), "Vibration analysis of functionally graded carbon nanotube-reinforced composite sandwich beams in thermal environment", *Adv. Aircr. Spacecr. Sci.* **5**(1), 107–128. <https://doi.org/10.12989/aas.2018.5.1.107>.
- Fantuzzi, N., Tornabene, F., Baccocchi, M. and Ferreira, A. (2018), "On the Convergence of Laminated Composite Plates of Arbitrary Shape through Finite Element Models", *J. Compos. Sci.*, **2**(1), 16. <https://doi.org/10.3390/jcs2010016>.
- Ferreira, A., Roque, C. and Martins, P. (2003), "Analysis of composite plates using higher-order shear deformation theory and a finite point formulation based on the multiquadric radial basis function method", *Compos. Part B Eng.*, **34**, 627–636. [https://doi.org/https://doi.org/10.1016/S1359-8368\(03\)00083-0](https://doi.org/https://doi.org/10.1016/S1359-8368(03)00083-0).
- Ferreira, A.J.M., Castro, L.M.S. and Bertoluzza, S. (2009), "A high order collocation method for the static and vibration analysis of composite plates using a first-order theory", *Compos. Struct.*, **89**(3), 424–432. <https://doi.org/10.1016/j.compstruct.2008.09.006>.
- Ferreira, A.J.M., Viola, E., Tornabene, F., Fantuzzi, N. and Zenkour, A.M. (2013), "Analysis of Sandwich Plates by Generalized Differential Quadrature Method", *Math. Probl. Eng.*, **2013**, 1–12. <https://doi.org/10.1155/2013/964367>.
- Foroutan, M., Moradi-Dastjerdi, R. and Sotoodeh-Bahreini, R. (2012), "Static analysis of FGM cylinders by a mesh-free method", *Steel Compos. Struct.*, **12**(1), 1–11.

- <https://doi.org/10.12989/scs.2011.12.1.001>.
- Ghanati, P. and Safaei, B. (2019), "Elastic buckling analysis of polygonal thin sheets under compression", *Indian J. Phys.*, **93**(1), 47–52. <https://doi.org/10.1007/s12648-018-1254-9>.
- Guessas, H., Zidour, M., Meradjah, M. and Tounsi, A. (2018), "The critical buckling load of reinforced nanocomposite porous plates", *Struct. Eng. Mech.* **67**(2), 115–123. <https://doi.org/http://dx.doi.org/10.12989/sem.2018.67.2.115>.
- Jalali M. H. Shahriari B, Zargar O, et al. (2018), "Free vibration analysis of rotating functionally graded annular disc of variable thickness using generalized differential quadrature method", *Sci. Iran.*, **25**(2), 728–740. <https://doi.org/10.24200/sci.2017.4325>.
- Jalali, M. H., Zargar, O. and Baghani, M. (2018), "Size-Dependent Vibration Analysis of FG Microbeams in Thermal Environment Based on Modified Couple Stress Theory", *Iran. J. Sci. Technol. Trans. Mech. Eng.* <https://doi.org/10.1007/s40997-018-0193-6>.
- Jalali, S.K. and Heshmati, M. (2016), "Buckling analysis of circular sandwich plates with tapered cores and functionally graded carbon nanotubes-reinforced composite face sheets", *Thin-Walled Struct.* **100**. <https://doi.org/10.1016/j.tws.2015.12.001>.
- Kamarian, S., Bodaghi, M., Pourasghar, A. and Talebi, S. (2017), "Vibrational behavior of non-uniform piezoelectric sandwich beams made of CNT-reinforced polymer nanocomposite by considering the agglomeration effect of CNTs", *Polym. Compos.* **38**, E553–E562. <https://doi.org/10.1002/pc.23933>.
- Lin, G., Zhang, P., Liu, J. and Li, J. (2018), "Analysis of laminated composite and sandwich plates based on the scaled boundary finite element method", *Compos. Struct.*, **187**, 579–592. <https://doi.org/10.1016/j.compstruct.2017.11.001>.
- Magnucka-Blandzi, E. (2008), "Axi-symmetrical deflection and buckling of circular porous-cellular plate", *Thin-Walled Struct.* **46**, 333–337. <https://doi.org/10.1016/j.tws.2007.06.006>.
- Mantari, J.L., Oktem, A.S. and Guedes Soares, C. (2011), "Static and dynamic analysis of laminated composite and sandwich plates and shells by using a new higher-order shear deformation theory", *Compos. Struct.*, **94**(1), 37–49. <https://doi.org/10.1016/j.compstruct.2011.07.020>.
- Mehar, K. and Panda, S.K. (2018), "Nonlinear finite element solutions of thermoelastic flexural strength and stress values of temperature dependent graded CNT-reinforced sandwich shallow shell structure", *Struct. Eng. Mech.*, **67**(6), 565–578. <https://doi.org/10.12989/sem.2018.67.6.565>.
- Mirzaalian, M., Aghadavoudi, F. and Moradi-Dastjerdi, R. (2019), "Bending Behavior of Sandwich Plates with Aggregated CNT-Reinforced Face Sheets", *J. Solid Mech.*, **11**(1), 26–38. <https://doi.org/10.22034/jsm.2019.664214>.
- Mohammadimehr M, Zarei HB, Parakandeh A, et al. (2017), "Vibration analysis of double-bonded sandwich microplates with nanocomposite facesheets reinforced by symmetric and un-symmetric distributions of nanotubes under multi physical fields", *Struct. Eng. Mech.* **64**(3), 361. <https://doi.org/10.12989/sem.2017.64.3.361>.
- Mohammadsalehi, M., Zargar, O. and Baghani, M. (2017), "Study of non-uniform viscoelastic nanoplates vibration based on nonlocal first-order shear deformation theory", *Meccanica*, **52**, 1063–1077. <https://doi.org/10.1007/s11012-016-0432-0>.
- Moradi-Dastjerdi, R. and Aghadavoudi, F. (2018), "Static analysis of functionally graded nanocomposite sandwich plates reinforced by defected CNT", *Compos. Struct.*, **200**, 839–848. <https://doi.org/10.1016/j.compstruct.2018.05.122>.
- Moradi-Dastjerdi, R. and Behdinan, K. (2019), "Thermoelastic static and vibrational behaviors of nanocomposite thick cylinders reinforced with graphene", *Steel Compos. Struct.* **31**(5), 529–539. <https://doi.org/10.12989/scs.2019.31.5.529>.
- Moradi-Dastjerdi, R. and Momeni-Khabisi, H. (2016), "Dynamic analysis of functionally graded nanocomposite plates reinforced by wavy carbon nanotube", *Steel Compos. Struct.* **22**(2), 277–299. <http://dx.doi.org/10.12989/scs.2016.22.2.277>.
- Moradi-Dastjerdi, R., Payganeh, G., Rajabizadeh Mirakabad, S. and Jafari Mofrad-Taheri, M. (2016), "Static and Free Vibration Analyses of Functionally Graded Nano- composite Plates Reinforced by Wavy Carbon Nanotubes Resting on a Pasternak Elastic Foundation", *Mech. Adv. Compos. Struct.*, **3**, 123–135. <https://doi.org/10.22075/mac.2016.474>.
- Moradi-Dastjerdi, R., Malek-Mohammadi, H. and Momeni-Khabisi, H. (2017), "Free vibration analysis of nanocomposite sandwich plates reinforced with CNT aggregates", *ZAMM - J. Appl. Math. Mech. / Zeitschrift fur Angew. Math. und Mech.* **97**(11), 1418–1435. <https://doi.org/10.1002/zamm.201600209>.
- Moradi-Dastjerdi, R., Payganeh, G. and Tajdari, M. (2018), "Thermoelastic Analysis of Functionally Graded Cylinders Reinforced by Wavy CNT Using a Mesh-Free Method", *Polym. Compos.*, **39**(7), 2190–2201. <https://doi.org/10.1002/pc.24183>.
- Neves, A.M.A., Ferreira, A.J., Carrera, E., Cinefra, M., Jorge, R.M.N. and Soares, C.M.M. (2012), "Static analysis of functionally graded sandwich plates according to a hyperbolic theory considering Zig-Zag and warping effects", *Adv. Eng. Softw.* **52**, 30–43. <https://doi.org/10.1016/j.advengsoft.2012.05.005>.
- Nguyen, K.T., Thai, T.H. and Vo, T.P. (2015), "A refined higher-order shear deformation theory for bending, vibration and buckling analysis of functionally graded sandwich plates", *Steel Compos. Struct.*, **18**(1), 91–120. <https://doi.org/10.12989/scs.2015.18.1.091>.
- Nguyen, N.V., Nguyen, H.X., Lee, S. and Nguyen-Xuan, H. (2018), "Geometrically nonlinear polygonal finite element analysis of functionally graded porous plates", *Adv. Eng. Softw.*, **126**, 110–126. <https://doi.org/10.1016/j.advengsoft.2018.11.005>.
- Polit, O., Anant, C., Anirudh, B. and Ganapathi, M. (2019), "Functionally graded graphene reinforced porous nanocomposite curved beams: Bending and elastic stability using a higher-order model with thickness stretch effect", *Compos. Part B*, **166**, 310–327. <https://doi.org/10.1016/j.compositesb.2018.11.074>.
- Pourasghar, A. and Chen, Z. (2016), "Thermoelastic response of CNT reinforced cylindrical panel resting on elastic foundation using theory of elasticity", *Compos. Part B Eng.*, **99**(15), 436–444. <https://doi.org/10.1016/j.compositesb.2016.06.028>.
- Pourasghar, A. and Chen, Z. (2019a), "Dual-phase-lag heat conduction in FG carbon nanotube reinforced polymer composites", *Phys. B Condens. Matter*, **564**, 147–156. <https://doi.org/10.1016/j.physb.2019.03.038>.
- Pourasghar, A. and Chen, Z. (2019b), "Effect of hyperbolic heat conduction on the linear and nonlinear vibration of CNT reinforced size-dependent functionally graded microbeams", *Int. J. Eng. Sci.*, **137**, 57–72. <https://doi.org/10.1016/j.ijengsci.2019.02.002>.
- Pourasghar, A. and Chen, Z. (2019c), "Hyperbolic heat conduction and thermoelastic solution of functionally graded CNT reinforced cylindrical panel subjected to heat pulse", *Int. J. Solids Struct.*, **163**, 117–129.
- Pourasghar, A. and Chen, Z. (2019d), "Nonlinear vibration and modal analysis of FG nanocomposite sandwich beams reinforced by aggregated CNTs", *Polym. Eng. Sci.*, <https://doi.org/10.1002/pen.25119>.
- Qin, Z., Pang, X., Safaei, B. and Chu, F. (2019), "Free vibration analysis of rotating functionally graded CNT reinforced composite cylindrical shells with arbitrary boundary conditions", *Compos. Struct.*, **220**, 847–860. <https://doi.org/10.1016/j.compstruct.2019.04.046>.
- Rad, A.B., Farzan-Rad, M.R. and Majd, K.M. (2017), "Static analysis of non-uniform heterogeneous circular plate with porous material resting on a gradient hybrid foundation involving friction force", *Struct. Eng. Mech.* **64**(5), 591. <https://doi.org/10.12989/sem.2017.64.5.591>.
- Rashidi, S., Esfahani, J.A. and Karimi, N. (2018), "Porous

- materials in building energy technologies—A review of the applications, modelling and experiments”, *Renew. Sustain. Energy Rev.* **91**, 229–247. <https://doi.org/10.1016/J.RSER.2018.03.092>.
- Reddy, J.N. (1993), *Introduction to the Finite Element Method*. McGraw-Hill, New York, USA.
- Reddy, J.N. (2004), *Mechanics of Laminated Composite Plates and Shells: Theory and Analysis*, CRC press, Florida, USA.
- Rezaiee-Pajand, M., Shahabian, F. and Tavakoli, F.H. (2012), “A new higher-order triangular plate bending element for the analysis of laminated composite and sandwich plates”, *Struct. Eng. Mech.*, **43**(2), 253–271. <https://doi.org/10.12989/sem.2012.43.2.253>.
- Safaei, B., Fattahi, A.M. and Chu, F. (2018), “Finite element study on elastic transition in platelet reinforced composites”, *Microsyst. Technol.*, **24**(6), 2663–2671. <https://doi.org/10.1007/s00542-017-3651-y>.
- Safaei, B., Moradi-Dastjerdi, R., Behdinin, K. and Chu, F. (2019), “Critical buckling temperature and force in porous sandwich plates with CNT-reinforced nanocomposite layers”, *Aerosp. Sci. Technol.*, **91**, 175–185. <https://doi.org/10.1016/j.ast.2019.05.020>.
- Safaei, B., Moradi-Dastjerdi, Rasool., Qin, Z., Behdinin, K. and Chu, F. (2019), “Determination of thermoelastic stress wave propagation in nanocomposite sandwich plates reinforced by clusters of carbon nanotubes”, *J. Sandw. Struct. Mater.*, <https://doi.org/10.1177/109963621984828>.
- Safaei, B., Moradi-Dastjerdi, Rasool., Qin, Z. and Chu, F. (2019), “Frequency-dependent forced vibration analysis of nanocomposite sandwich plate under thermo-mechanical loads”, *Compos. Part B Eng.* **161**, 44–54. <https://doi.org/10.1016/j.compositesb.2018.10.049>.
- Safaei, B., Moradi-Dastjerdi, R., Behdinin, K., Qin, Z. and Chu, F. (2019), “Thermoelastic behavior of sandwich plates with porous polymeric core and CNT clusters/polymer nanocomposite layers”, *Compos. Struct.*, **226**. <https://doi.org/10.1016/j.compstruct.2019.111209>.
- Salami, S.J. and Dariushi, S. (2018), “Analytical, numerical and experimental investigation of low velocity impact response of laminated composite sandwich plates using extended high order sandwich panel theory”, *Struct. Eng. Mech.* **68**(3), 325–334. <https://doi.org/10.12989/sem.2018.68.3.325>.
- Setoodeh, A.R., Shojaee, M. and Malekzadeh, P. (2019), “Vibrational behavior of doubly curved smart sandwich shells with FG-CNTRC face sheets and FG porous core”, *Compos. Part B Eng.*, **165**, 798–822. <https://doi.org/10.1016/J.COMPOSITESB.2019.01.022>.
- Shokri-Ooijghaz R, Moradi-Dastjerdi, R., Mohammadi, H. and Behdinin, K. (2019), “Stress distributions in nanocomposite sandwich cylinders reinforced by aggregated carbon nanotube”, *Polym. Compos.*, **40**(S2), E1918–E1927. <https://doi.org/10.1002/pc.25206>.
- Thai, C. H., Ferreira, A. J. M., Carrera, E. and Nguyen-Xuan, H. (2013), “Isogeometric analysis of laminated composite and sandwich plates using a layerwise deformation theory”, *Compos. Struct.*, **104**, 196–214. <https://doi.org/10.1016/j.compstruct.2013.04.002>.
- Tian, A., Ye, R. and Chen, Y. (2016), “A new higher order analysis model for sandwich plates with flexible core”, *J. Compos. Mater.*, **50**(7), 949–961. <https://doi.org/10.1177/0021998315584650>.
- Tornabene, F., Fantuzzi, N., Baccocchi, M. and Reddy, J.N. (2017), “A posteriori stress and strain recovery procedure for the static analysis of laminated shells resting on nonlinear elastic foundation”, *Compos. Part B Eng.*, **126**, 162–191. <https://doi.org/10.1016/J.COMPOSITESB.2017.06.012>.
- Tornabene, F., Fantuzzi, N. and Baccocchi, M. (2017), “Linear Static Behavior of Damaged Laminated Composite Plates and Shells”, *Materials (Basel)*, **10**(7), 811. <https://doi.org/10.3390/ma10070811>.
- Vinson, J.R. (2001), “Sandwich Structures”, *Appl. Mech. Rev.* **54**(3), 201. <https://doi.org/10.1115/1.3097295>.
- Wang, Z. and Shen, H. (2012), “Nonlinear vibration and bending of sandwich plates with nanotube-reinforced composite face sheets”, *Compos. Part B*, **43**(2), 411–421. <https://doi.org/10.1016/j.compositesb.2011.04.040>.
- Xiang, S., Wang, Y.G. and Kang, G.W. (2015), “Static Analysis of Laminated Composite Plates Using n -Order Shear Deformation Theory and a Meshless Global Collocation Method”, *Mech. Adv. Mater. Struct.*, **22**(6), 470–478. <https://doi.org/10.1080/15376494.2013.799247>.
- Xiaohui, R., Zhen, W. and Bin, J. (2018), “A refined sinusoidal theory for laminated composite and sandwich plates A refined sinusoidal theory for laminated composite and sandwich plates”, *Mech. Adv. Mater. Struct.*, <https://doi.org/10.1080/15376494.2018.1538469>.
- Zarei, A. and Khosravifard, A. (2019), “A meshfree method for static and buckling analysis of shear deformable composite laminates considering continuity of interlaminar transverse shearing stresses”, *Compos. Struct.*, **209**, 206–218. <https://doi.org/10.1016/j.compstruct.2018.10.077>.
- Zargar, O., Masoumi, A. and Moghaddam, A.O. (2017), “Investigation and optimization for the dynamical behaviour of the vehicle structure”, *Int. J. Automot. Mech. Eng.*, **14**, 4196–4210. <https://doi.org/10.15282/ijame.14.2.2017.7.0336>.
- Zhao, J., Xie, F. and Wang, A. (2019), “Vibration behavior of the functionally graded porous (FGP) doubly-curved panels and shells of revolution by using a semi-analytical method”, *Compos. Part B*, **157**, 219–238. <https://doi.org/10.1016/j.compositesb.2018.08.087>.

CC

Appendix

The components of elastic constant matrix \mathbf{D} for isotropic porous layer can be determined as:

$$\begin{aligned} D_{11} = D_{22} &= \frac{E_p}{1-\nu_p^2}, D_{12} = \nu_p D_{11}, \\ D_{44} = D_{55} = D_{66} &= G_p, D_{16} = D_{26} = D_{45} = 0 \end{aligned} \quad (\text{A1})$$

where G_p is shear modulus of porous layer.

Due to the elimination of σ_z in shear deformation plate theories and presenting high accurate results, the reduced elastic constant matrix for the laminated composite layers should be considered. The components of such reduced matrix D_{ij} can be determined as below:

$$D_{ij} = \begin{cases} \bar{Q}_{ij} - (\bar{Q}_{i3} \cdot \bar{Q}_{j3}) / Q_{33} & i, j = 1, 2, 6 \\ \bar{Q}_{ij} & i, j = 4, 5 \end{cases} \quad (\text{A2})$$

where

$$\begin{aligned} Q_{11} &= E_1 \frac{1-\nu_{23}\nu_{32}}{\Delta}, Q_{22} = E_2 \frac{1-\nu_{13}\nu_{31}}{\Delta} \\ Q_{12} &= E_1 \frac{\nu_{21} + \nu_{31}\nu_{32}}{\Delta}, Q_{13} = E_3 \frac{\nu_{13} + \nu_{12}\nu_{23}}{\Delta} \\ Q_{23} &= E_3 \frac{\nu_{23} + \nu_{13}\nu_{21}}{\Delta}, Q_{33} = E_3 \frac{1-\nu_{12}\nu_{21}}{\Delta} \\ Q_{44} &= G_{23}, Q_{55} = G_{13}, Q_{66} = G_{12} \\ \Delta &= \frac{1-\nu_{32}\nu_{23} - \nu_{21}\nu_{12} - \nu_{13}\nu_{31} - 2\nu_{32}\nu_{21}\nu_{13}}{E_1 E_2 E_3} \end{aligned} \quad (\text{A3})$$

The other important parameter on the elastic constants of laminated composites is the angle of fibers α in each layer. The components of elastic matrix for these composite layers \bar{Q}_{ij} can be determined as (Reddy 2004):

$$\begin{aligned} \bar{Q}_{11} &= m^4 Q_{11} + 2m^2 n^2 (Q_{12} + 2Q_{66}) + n^4 Q_{22}, \\ \bar{Q}_{22} &= n^4 Q_{11} + 2m^2 n^2 (Q_{12} + 2Q_{66}) + m^4 Q_{22}, \\ \bar{Q}_{44} &= m^2 Q_{44} + n^2 Q_{55}, \bar{Q}_{55} = m^2 Q_{55} + n^2 Q_{44}, \\ \bar{Q}_{66} &= -m^2 n^2 (Q_{11} + Q_{22} - 2Q_{12}) + (m^4 - n^4) Q_{66}, \\ \bar{Q}_{12} &= m^2 n^2 (Q_{11} + 4Q_{22} Q_{66}) + (m^4 + n^4) Q_{12}, \\ \bar{Q}_{13} &= m^2 Q_{13} + n^2 Q_{23}, \bar{Q}_{23} = n^2 Q_{13} + m^2 Q_{23}, \\ \bar{Q}_{36} &= (Q_{32} - Q_{31}) mn, \bar{Q}_{45} = (Q_{45} - Q_{55}) mn, \\ \bar{Q}_{16} &= -mn [n^2 Q_{11} - m^2 Q_{22} - (m^2 - n^2)(Q_{12} + 2Q_{66})] \\ \bar{Q}_{26} &= -mn [m^2 Q_{11} - n^2 Q_{22} - (m^2 - n^2)(Q_{12} + 2Q_{66})] \end{aligned} \quad (\text{A4})$$

where $m = \cos \alpha$ and $n = \sin \alpha$.